Inelastic nuclear screening for different secondaries produced in p+Pb collisions at LHC energy

Carlos Merino
University of Santiago de Compostela
Galiza-Spain

in collaboration with
G.H. Arakelyan, Yu.M. Shabelski, and A.G. Shuvaev

carlos.merino@usc.es

Outline:

- Aim
- Formalism of the Quark-Gluon String Model: inclusive spectra in pp and pA collisions
- Very high energy collisions: inelastic screening (percolation) effects
- Results: rapidity spectra of different secondaries at LHC energies
- Conclusions

Phys. Rev. D95, 074013 (2017), and references therein

Aim:

To calculate in the frame of the Quark-Gluon String Model the inclusive spectra of secondaries, produced in soft (minimum bias) pPb collisions at LHC energy, by taking into account the inelastic screening corrections (percolation effects).

These effects should be quite large at very high energies.

Formalism of the Quark-Gluon String Model: inclusive spectra in pp and pA collisions:

- The Quark-Gluon String Model (QGSM) is based on Dual Topological Unitarization, Regge Phenomenology, and nonperturbative features of QCD.

- The QGSM successfully describes multiparticle production in hadron-hadron and hadron-nucleus collisions.

- **High energy interactions proceed via the exchange of one or several Pomerons, and elastic and inelastic processes result from cutting between or through Pomerons.**

- **The inclusive spectra of hadrons are related to the corresponding fragmentation functions of quarks and diquarks, constructed by using Reggeon counting rules.**

- **For the description of interactions with a nuclear target, the Gribov-Glauber theory is used. The interaction is considered as the superposition of interactions with different numbers of target nucleons.**

The inclusive spectrum of a secondary hadron **h** is determined by the convolution of the diquark, valence quark, and sea quark distributions, $u(x, n)$, in the incident particles, with the fragmentation functions, $G^h(z)$, of quarks and diquarks into the secondary hadron **h**.

Both the distributions and the fragmentation functions are constructed using the Reggeon counting rules.

Each exchanged Pomeron corresponds to a cylindrical diagram.

When cutting one Pomeron, two showers of secondaries are produced

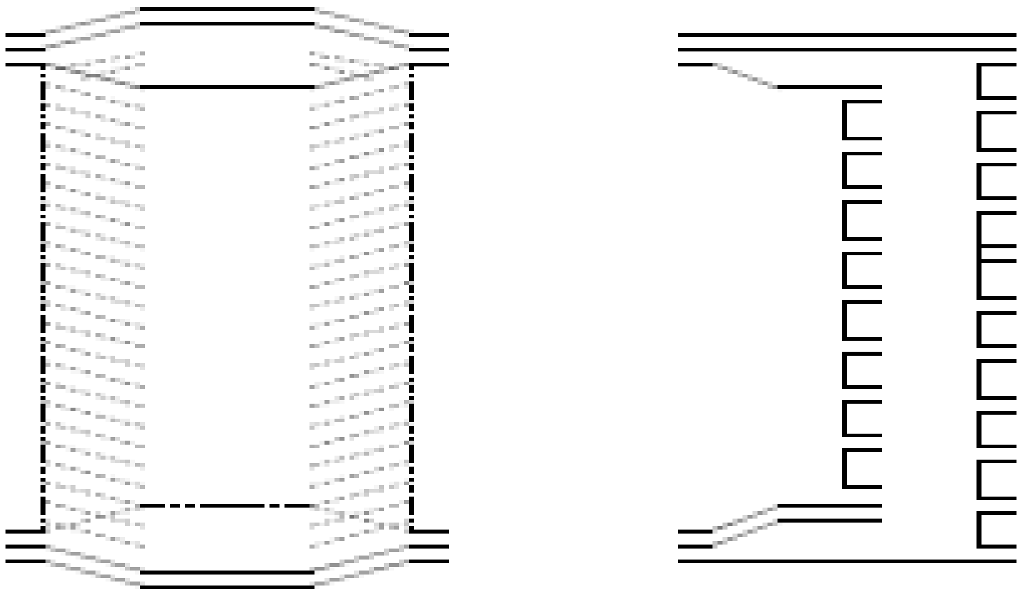

In the case of multipomeron exchange, the distributions of valence quarks and diquarks are softened due to the appearance of a sea quark contribution.

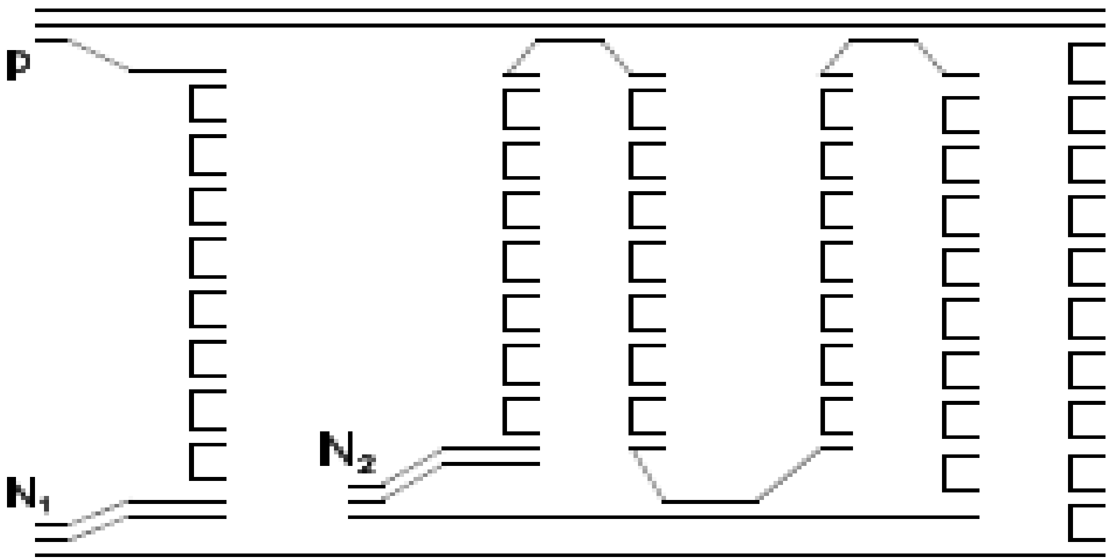

Every distribution $u_i(x, n)$ is normalized to unity.

For a nucleon target, the inclusive rapidity, **y**, or Feynman-x, x_F , spectrum of a secondary hadron **h** has the form

$$\frac{dn}{dy}=\frac{x_E}{\sigma_{inel}}\cdot\frac{d\sigma}{dy}=\sum_{n=1}^{\infty}\omega_n\cdot\Phi_n^h(x)$$

where the functions $\Phi_n^h(x)$ determine the contribution of diagrams with **n** cut Pomerons, ω_n is the relative weight of these diagrams (we neglect the numerically small contribution of diffraction dissociation processes).

For pp collisions:

$$\phi_n^h(x) = f_{qq}^h(x_+,n)\cdot f_q^h(x_-,n) + f_q^h(x_+,n)\cdot f_{qq}^h(x_-,n) + 2(n-1) f_s^h(x_+,n)\cdot f_s^h(x_-,n) \ ,$$

$$x_\pm = \frac{1}{2}\left[\sqrt{4m_T^2/s + x^2} \pm x\right] \ ,$$

where f_{qq}, f_q, and f_s are the contributions of diquarks, valence quarks, and sea quarks, respectively.

These contributions are determined by the convolution of the diquark and quark distributions with the fragmentation functions, e.g.,

$$f_q^h(x_+, n) = \int_{x_+}^1 u_q(x_1, n) \cdot G_q^h(x_+/x_1) dx_1 \quad .$$

The diquark and quark distributions, as well as the fragmentation functions are determined by Regge asymptotics.

In the case of interaction with a nuclear target, the Gribov-Glauber theory is used (superposition of interactions with different numbers of target nucleons).

Let $W_{pA}(\nu)$ be the probability for the inelastic interactions of the proton with ν nucleons of the target, and σ^{pA}_{prd} the total cross section of secondary production in a proton-nucleus collision:

$$W_{pA}(\nu) = \sigma^{(\nu)} / \sigma^{pA}_{prod} \, ,$$

$$\sigma^{(\nu)} = \frac{1}{\nu!} \int d^2b \cdot [\sigma^{pN}_{inel} \cdot T(b)]^{\nu} \cdot e^{-\sigma^{pN}_{inel} \cdot T(b)}$$

$$\sigma^{pA}_{prod} = \int d^2b \cdot \left(1 - e^{-\sigma^{pN}_{inel} \cdot T(b)}\right) ,$$

where T(b) is the profile function of the nuclear target:

$$T(b) = A \int_{-\infty}^{\infty} dz \cdot \rho(b, z) ,$$

with ρ, the one-particle nuclear density.

The average value of ν has the form:

$$\langle \nu \rangle = \frac{A \cdot \sigma^{pp}_{inel}}{\sigma^{pA}_{prod}} .$$

$$\langle \nu \rangle_{p+Pb} \approx 7.9.$$

Very high energy collisions: inelastic screening (percolation) effects

The QGSM model gives a reasonable description of the inclusive spectra of different secondaries produced at low and intermediate (compared to RHIC and LHC) energies.

At RHIC energies, the situation changes (see detailed discussion by Capella, Kaidalov, and Tran, 1999): the midrapidty values of the theoretical inclusive densities for Pb-Pb collisions without saturation effects are a factor 2 larger than when taking into account those effects (experimentally confirmed by Au-Au RHIC data).

This suppression can be explained by the inelastic screening corrections connected to multipomeron interactions.

The calculations of inclusive densities and multiplicities, both in pp, and in heavy ion collisions, with accounting of inelastic nuclear screening, can be done in the percolation theory.

The percolation model also provides a reasonable description of transverse momentum distributions (at low and intermediate p_T), including the Cronin effect and the behaviour of the baryon/meson ratio.

Percolation approach: given a certain transverse radius for the Pomeron, when the number of Pomerons in the interaction region increases, some of them overlap in the transverse space, and they fuse in a single Pomeron.

As a result, the internal partons can split (saturation of the final inelastic density).

In order to account for the percolation effects in the QGSM, one considers in the central region the maximal number of Pomerons emitted by a nucleon, n_{max}, and the contribution of all the diagrams with $n \leq n_{max}$ are accounted for. By doing this, all calculations become rather simple.

The QGSM fragmentation allows one to calculate the spectra of secondaries integrated over p_T, as functions of initial energies, rapidity, and x_F.

A good agreement with the RHIC data on the inclusive spectra of secondaries is obtained with a value $n_{max} = 13$. By normalizing to the midrapidity ALICE data at $\sqrt{s} = 5 TeV$, we obtain $n_{max} = 21$ (the number of strings increases with the initial energy, even when the percolation effects are included).

The predictive power of our calculation lies on the fact that if inelastic nuclear screening comes mainly from the Pomeron interactions, the screening effects should basically be the same for all the secondaries.

One additional effect has also been taken into account in our calculations: the baryon charge transfer to large distances in rapidity space, through the string junction (SJ) effect.

The SJ mechanism leads to an asymmetry in the production of baryons and antibaryons in the central region. This asymmetry is nonzero even at LHC energies.

Results: rapidity spectra of different secondaries at LHC energies

First, we present the QGSM description of $\pi^{\pm}$, $K^{\pm}$, p, and $\bar{p}$ productions in pp collisions at LHC energies, and we compare with data by CMS (2012, 2014), and by ALICE collaborations (2011, 2014, 2015).

Though the 20-30% disagreement between ALICE and CMS data, the QGSM result is qualitatively compatible with both samples.

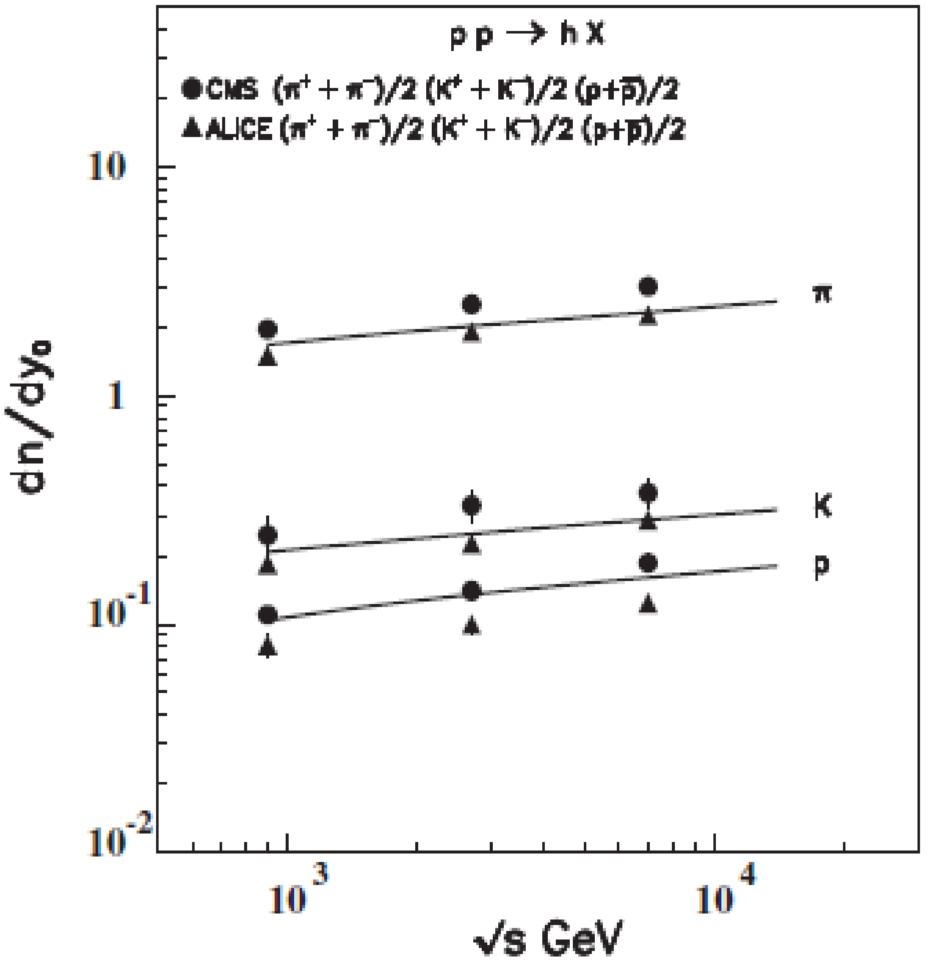

We have also compared our results with the experimental data for p+Pb collisions by the CMS Collaboration (2014), on the inclusive densities of $\pi^{\pm}, K^{\pm}, p$, and $\bar{p}$.

The inelastic nuclear screening factor is little larger than 2, and practically the same for all considered secondaries.

particles	CMS Collaboration dn/dy, $\lvert y\rvert \le 1$ [5]	QGSM p+Pb	QGSM pp	QGSM r
π^+	8.074 ± 0.087	8.103	2.190	3.70
π^-	7.971 ± 0.079	7.923	2.147	3.69
K^+	1.071 ± 0.069	1.006	0.273	3.69
K^-	0.984 ± 0.047	0.996	0.271	3.66
p	0.510 ± 0.018	0.545	0.150	3.63
$\bar{p}$	0.494 ± 0.017	0.536	0.148	3.62

We also present our results for hyperon and antihyperon production in pp and p+Pb collisions at $\sqrt{s}=5\,TeV$.

particles	$p+\text{Pb}\ dn/dy_{y=0}$	$\text{pp}\ dn/dy_{y=0}$	r
Λ	0.307	0.0843	3.64
$\bar{\Lambda}$	0.303	0.0827	3.66
Ξ^-	0.0250	0.00676	3.70
$\bar{\Xi}^+$	0.0248	0.00669	3.70
Ω^-	0.00143	0.000401	3.57
$\bar{\Omega}^+$	0.00142	0.000397	3.58

The ratios of the inclusive densities of all secondary hyperons and antihyperons produced on Pb and hydrogen targets are practically the same as for secondary meson production, with a 5% accuracy.

Conclusions (1)

- The Quark-Gluon String Model is a phenomenological model based on rigorous theoretical background.

- QGSM conceptually differs from QCD-based parton models, that are more adequate at small distances (high Q^2), and from Monte-Carlo models, which contain many parameters of unknown values.

- The QGSM calculations show that inelastic screening corrections at LHC energies are really large. For all the ratios of inclusive densities of the secondaries produced in lead and hydrogen targets

$$r\left(\frac{p+Pb}{pp}\right)=3.6-3.7\ ,$$

instead of the expected value without screening, **r= 7.5-8.0**.

Conclusions (2)

- The QGSM approach for high energy inelastic pp, p-nucleus, and nucleus-nucleus collisions with multiparticle production provides a natural explanation of the independence of the nuclear screening effects on the type of the produced particles in the central region of the inclusive spectrum.

- If confirmed experimentally, this would indicate that the interaction of secondaries in the final state would be small.